Electrical Tomography as laboratory monitoring tool

Electrical Tomography as laboratory monitoring tool

Cesare Comina,* Renato Maria Cosentini,** Sebastiano Foti,*** Guido Musso****

Summary

Electrical Resistivity Tomography (ERT) has proved to be a powerful technique for investigating pore fluid properties and soil characteristics in different field applications. In this respect, ERT is often used in geophysics to reconstruct geological horizons and to monitor the flow of contaminants, providing information on their spatial scattering and on the location of contamination sources. Interesting results have been recently obtained also at the laboratory scale, showing the potential of ERT as a subsidiary imaging tool for the characterization of soil samples.

ERT methods are relatively cost effective and fast in terms of data acquisition. Advantages of the technique rely on the fact that the electrical conductivity of soil can be related to the physico-chemical properties of the soil-water mixture (concentration of ionic species, porosity, tortuosity, specific surface, cation exchange capacity). Therefore, at least in principle, ERT results can be used not only for imaging purposes, but they can be as well interpreted from a quantitative point of view, aiding in the characterization of transport parameters.

Within this context, this paper presents the results of some laboratory tests designed to explore the potentiality of 3D ERT with respect to phenomena of interest in geotechnical engineering. Tests have been executed within an innovative oedometer cell, equipped both for the execution of high speed 3D electrical tomography and for the measurement of compressional and shear waves velocities which can provide an independent monitoring tool. Results concerning changes of the saturation degree, one dimensional consolidation and salt diffusion processes are reported.

Keywords: Non invasive laboratory tests, saturation, consolidation, diffusion

1. Introduction

Electrical conductivity measurements have been used in the past to characterize the state of soil samples with success. The electrical conductivity of a porous media is related to the electrical conductivity of the constituent phases, and to its saturation, fabric and porosity [see e.g. ARCHIE, 1942; PFANNKUCH, 1969; BERRYMAN, 1995; MUALEN and FRIEDMAN, 1991]. Therefore, the evaluation of electrical conductivity can provide valuable information about the soil state.

For example, electrical measurements in the lab have been used to estimate the evolution of the saturation degree in column tests of pollutant filtration [KAMON *et al.*, 2003], to monitor processes of sedimentation and consolidation [MCCARTER and DESMAZES, 1997; BLEWETT *et al.*, 2001, MCCARTER *et al.*, 2005], to evaluate the diffusion of salts in saturated samples [SHACKELFORD *et al*, 1999]. Such investigations were limited to one-dimensional conditions and mostly based on punctual or averaged measurements, while no estimations of the variability of the electrical conductivity distribution inside of the specimens, associated to local variations of soil characteristics, was available.

An attempt to overcome this limitation is offered by the Electrical Resistivity Tomography (ERT). With this technique, the local distribution of the electrical conductivity is reconstructed on the basis of a large number of external measurements and of the subsequent solution of the inverse problem. With such approach, the spatial distribution of the electrical conductivity within the object is obtained. The repetition of measurements and reconstructions at different times allows tracking the evolution of the electrical conductivity field, improving the efficiency in monitoring processes such as the ones cited above.

Although ERT is widely adopted in geophysical prospecting, its use in the laboratory is at the moment scarce and limited mostly to 2D geometries. Reconstructions are typically performed on planar sections located in the central part of the sample. Among the processes that have been monitored in these conditions we can cite saline diffusion from punctual sources in reconstituted sand samples

* Assistant Professor, Dipartimento di Scienze della Terra, Università degli Studi di Torino
** Research Associate, Dipartimento di Ingegneria Strutturale e Geotecnica, Politecnico di Torino
*** Assistant Professor, Dipartimento di Ingegneria Strutturale e Geotecnica, Politecnico di Torino
**** Assistant Professor, Dipartimento di Ingegneria Strutturale e Geotecnica, Politecnico di Torino

[COMINA *et al.*, 2005; DAMASCENO *et al.*, 2009] and one dimensional solute transport in undisturbed soil columns [BINLEY *et al.*, 1996]. Information on the true 3D diffusion process deduced from these observations is necessarily qualitative. Indeed, while the reconstructed electrical conductivity values are assigned to a plane section, the electric flow lines generated by the electrodes are not constrained to the same plane. In fact, the reconstruction is affected as well by the conductivity of the soil mass outside that plane.

The evolution towards full 3D electrical conductivity monitoring of transient phenomena can then greatly improve the usefulness of the technique, but it introduces the following requirements:

- the electrode distribution around the sample must be designed carefully to allow for a complete characterization of the specimen, including the center of the sample where the sensitivity of the inverse problem is poorer;
- a fast acquiring device and a correct choice of the measuring sequence are necessary in order to effectively monitor transient phenomena. The acquisition time is indeed proportional to the square of the number of electrodes and a correct 3D reconstruction requires a higher number of measurements than a 2D reconstruction, in order to correctly image a sample;
- as a consequence of the non linearity of the inverse problem, an optimization of the inversion software is required to make the problem cost and time effective.

This paper presents preliminary results of 3D laboratory imaging of different transient processes. Phenomena considered include the evolution of sample saturation, the monitoring of oedometer tests, and of the diffusion of a saline solution. All the tests have been executed on homogeneous samples. The equipment used for the experimental program is briefly presented in the next section.

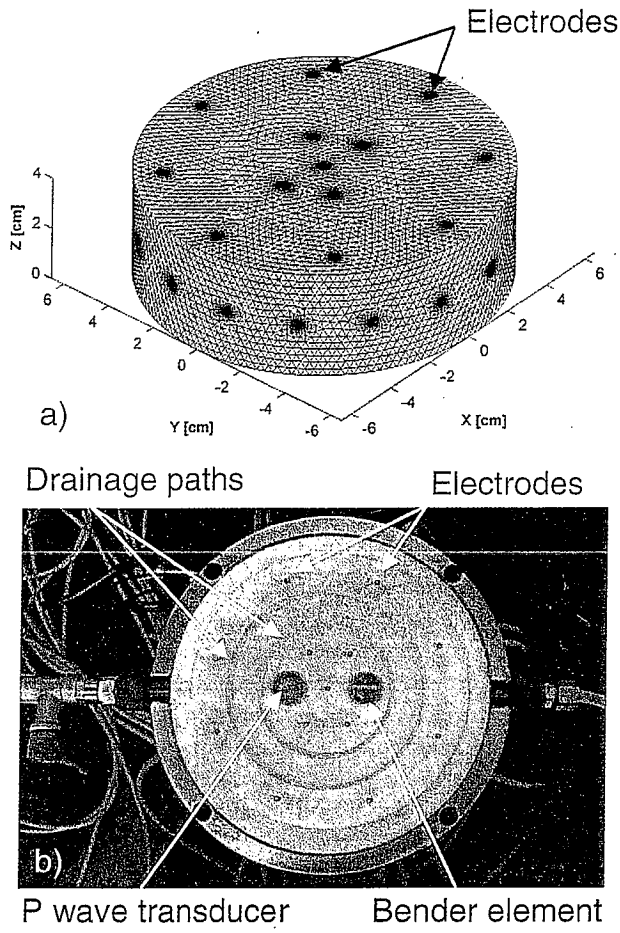

Fig. 1(a) – The 3D mesh used in the reconstructions with evidence of the disposition of electrodes; (b) picture of the oedometer base showing the location of water drainages, electrodes and seismic sensors.

Fig. 1(a) – Mesh 3D usata nelle ricostruzioni con evidenza della disposizione degli elettrodi; (b) base dell'edometro con indicazione del sistema di drenaggio, degli elettrodi e dei sensori di onde sismiche.

2. Instrumentation

An oedometer cell has been specifically designed in order to perform 3D ERT and to measure the velocity of compression (P) and shear (S) seismic waves together with conventional external measurements [COMINA *et al.*, 2008].

In this apparatus both the variations of the electrical property of soil specimens, by means of the reconstruction of the inner conductivity field, and the concomitant changes in the mechanical characteristics, by means of external load-displacement measurements and small-strain moduli, can be monitored accurately. This paper mainly focuses on the results of electrical tomography since it is an innovative technique in laboratory apparatuses, while only some shear and compression velocity data are presented with reference to the effect that the saturation degree can have on wave propagation providing an insight of possible combined use of the two measures.

The oedometer cell has an internal diameter of 130 mm and can host samples with height from 20 to 60 mm. Most electrodes dispositions for 3D tomography are organized with parallel rings of electrodes at different heights along the lateral boundaries of the sample. In the present study, a non conventional disposition has been preferred, with electrodes both on the sidewall and on the top and bottom bases (Fig. 1b). This setup gives a large amount of information in the center of the sample, where the resolution of the inverse problem is usually poor [LIONHEART *et al.*, 2001]. All together, 42 electrodes having a diameter of 1 mm are placed upon the external boundary of the soil sample (16 electrodes at

regular spacing along the sidewall at a height of 2 cm from the bottom base and 13 electrodes on each base). The soil sample is completely insulated from the confining stainless steel of the cell by means of a high resistivity material that prevents short circuiting of the electrodes. For the same reason, particular care is posed to have fully insulated water flow paths. Due to the impossibility of using porous stones on the bases, drainage is permitted by concentric rings of the insulating material having a tolerance of few microns between them (Fig. 1b).

The Complex Impedance Tomograph (Fig. 2) used for injecting currents and acquiring potentials has been constructed by the company Iridium Italy. It is a very fast acquiring device with a 16 bit resolution. The instrument can perform approximately 200 acquisitions per second (at an operating frequency of 1 kHz) so that it is possible to correctly appreciate water content or concentration variations inside samples also for relatively fast transitory phenomena. The tomograph is connected to the electrodes of the cell by means of three multiplexers (one for the circumferential electrodes the other two respectively for top and bottom bases). The electrical measurements are performed on basis of a four point measurements scheme. Electrodes placed on the sidewall and on the bases are used alternatively to inject current and to measure the electrical potential. The measurement protocol combines different acquisition schemes: 'horizontal' measurements, in which the electrodes injecting the electrical current and those measuring the potential are on the sidewall; 'vertical' measurements, in which the electrodes injecting the electrical current and those measuring the potential are on the bases; 'mixed' measurements, where the electrodes injecting the current are on the sidewall and the electrodes measuring the potential are on the bases.

After performing a large enough number of independent measurements, the distribution of the electrical conductivity within the sample is estimated with a reconstruction procedure done with a commercial software developed by sc-aip (www.sc-aip.com), which uses a least-squares algorithm with a Tikhonov regularization inversion technique. In the reconstructions the choice of the reguralization parameter plays an important role. Indeed if on one side it reduces the model variance, thus helping to obtain a stable solution, on the other hand it reduces as well the resolution. It can be proved that a solution able to reduce model variance and increase its resolution at the same time does not exist [MENKE, 1984; TARANTOLA, 2005]. Thus the choice of the optimal regularization factor requires a trial and error procedure looking for conductivity distributions that are consistent with the physical process under investigation.

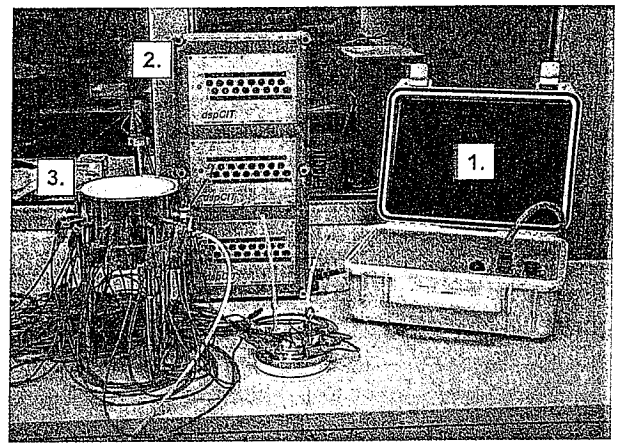

Fig. 2 – Measurement set-up: 1. Complex Impedance Tomograph; 2. Multiplexer and connection to the cell; 3. EIT-edometer cell.
Fig. 2 – Strumentazione: 1. Complex Impedance Tomograph; 2. Multiplexer e connessione alla cella; 3. Cella edometrica EIT-edometer.

The forward algorithm implemented within the software evaluates the current flow generated from the electrodes, which are modeled using their real dimensions [Complete Electrode Model methodology – SOMERSALO *et al.*, 1992] with a mesh refinement around them (Fig.1a). In the reconstruction, the electrical conductivity is a scalar quantity, assuming the isotropy of the electrical properties.

Full details about instrumentation and reconstruction software can be found in COMINA *et al.* [2008], together with the characteristics of the sensors to measure P and S wave velocity which are hosted in the top and bottom bases of the cell (Fig. 1b).

3. Unsaturated soil test

The electrical conductivity of a soil is a function of the electrical conductivity of its constituents, its porosity and its fabric. Depending on the assumptions on the electrical behavior of the solid phase, theoretical models can be divided into 'non conductive particle models' and 'conductive particle models' [MITCHELL and SOGA, 2005]. In general, the solid phase can be reasonably assumed to be non conductive for coarse soils and for fine soils with low specific surface and natural salt contents [SANTAMARINA, 2001].

Among the 'non conductive particle models', Archie's law (1942) is the most widely used. It has been derived for oil reservoir sands, and in fully saturated conditions it can be written as:

$$\sigma_T = \sigma_w n^m \qquad (1)$$

where σ_T is the electrical conductivity of the soil, σ_w is the electrical conductivity of the water phase, n is

the porosity and m is an exponent that accounts for the tortuosity of the porous medium (and therefore its fabric).

The effect of saturation is then accounted for by a power law, function of the saturation degree S_r:

$$\sigma_T = \sigma_w n^m S_r^p \qquad (2)$$

where the empirical exponent p has been found to depend as well on the fabric of the material, and particularly on its pore size distribution [see e.g. the work of SEN, 1997].

Therefore, when the porosity and the fabric of the soil and the electrical conductivity of the pore water are kept constant, a reduction of the water content involves a progressive decrease of conductivity and vice versa. Note that, in the petroleum engineering literature, Archie's law is usually expressed in terms of electrical resistivity. The formulation in terms of electrical conductivity is more common in geotechnical literature [see e.g. MITCHELL and SOGA, 2005]. This approach, besides respecting the formalism of the theory of irreversible processes [YEUNG, 1990], is more intuitive, since it ensures that the variations of the physical variables (porosity, saturation and chemical concentration) and of the electrical term occur in the same direction.

An experiment has been conduced on homogeneous sand samples to evaluate the potentiality of ERT reconstruction in distinguishing saturation changes. Samples have been statically compacted at an average porosity $n = 0.4$ and at different initial mass water contents corresponding to different saturation degrees. A 0.1 M KCl water solution was used as the liquid phase, ensuring constant σ_w values.

ERT has been performed for each sample (results in Fig. 3). The value of the regularization parameter adopted for this test ($\alpha = 1 \times 10^{-2}$) results from a series of trial inversions of each sample obtained by changing the regularization parameter in the range from 10^{-1} to 10^{-4}. The same value has then been adopted for all the reconstructions, in order not to introduce artifacts in the inversion. The increase of the soil conductivity with saturation can be appreciated. The images show an almost homogeneous distribution of conductivity at each stage, reflecting the uniformity of the sand specimen. It is however possible to distinguish some zones of the specimen in which variations in conductivities are observed, reflecting local heterogeneities of porosity and/or saturation. These results show that an analysis of conductivity distribution within the sample could provide an idea of how the de-saturation or saturation processes are evolving.

Interpretation of results in the light of equation (2) has been done by relating, at any water content,

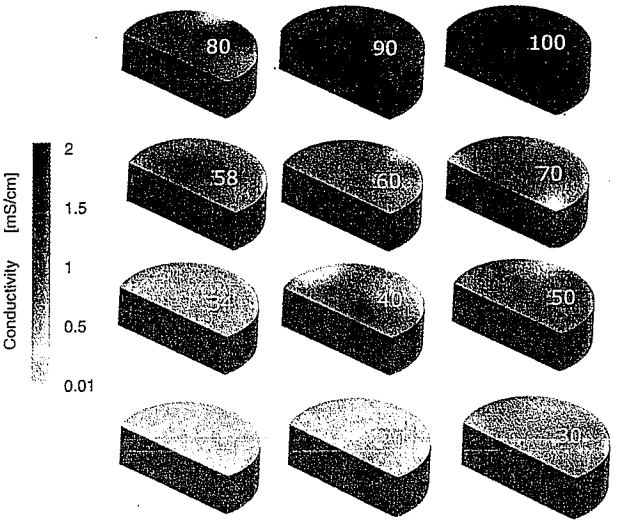

Fig. 3 – Unsaturated soil test: tomographic reconstructions of sand sample at different saturation degrees.
Fig. 3 – Prova su terreno non saturo: ricostruzioni tomografiche dei campioni di sabbia a differenti valori del grado di saturazione.

the average conductivity σ_T of the specimen to the corresponding saturation degree S_r. The m and p exponents were found to be equal respectively to 2.28 and 1.64, values in agreement with published results for similar materials. In figure 4 the reconstructed conductivities, averaged over the sample volume, and the predictions of Archie's law are reported in a non dimensional form, introducing a relative electrical conductivity as the ratio $\sigma_T(S_r) / \sigma_T(S_r = 1)$. The choice of a constant m for all the saturation degrees and of the power law S_r^p when accounting for the influence of saturation seems to be quite substantiated for the soil under investigation.

Water retention characteristics of the soil have been obtained by the filter paper method [ASTM D 5298-94]. The experimental data fitted with the Van Genuchten equation (1980) are showed in figure 5. The combined analysis of the results of figures 4 and 5 suggests that, under known porosity conditions, the calibration of ERT results together with devoted water retention curves could be used in principle to estimate suction in unsaturated soils. It must be outlined that this approach should be followed with some caution. Indeed, mineralogical and microstructural issues affecting the electrical conductivity of a geological material are many (accounted in different manners by different models, see e.g. WAXMAN and SMITS [1968] for the role of surface conductance, and SEN [1997] for the role of inclusions and of bimodal pore size distributions). Moreover, water retention properties depend on several factors, such as void ratio, clay content, pore size distribution, pore fluid salinity and on the direction of the hydraulic path. In clean sands such as the one stud-

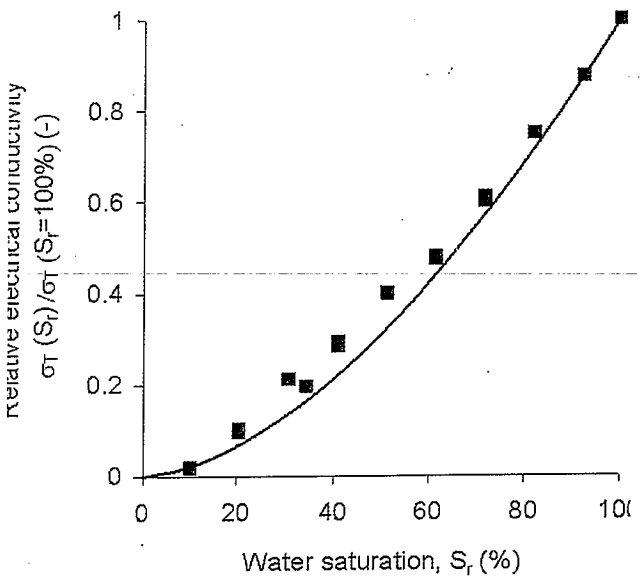

Fig. 4 – Unsaturated soil test: relative electrical conductivity versus water saturation curve of the sand considered in the wetting tests.

Fig. 4 – Prova su terreno non saturo: diagramma della conducibilità elettrica relativa in funzione della saturazione per la sabbia utilizzata nella prova di imbibizione.

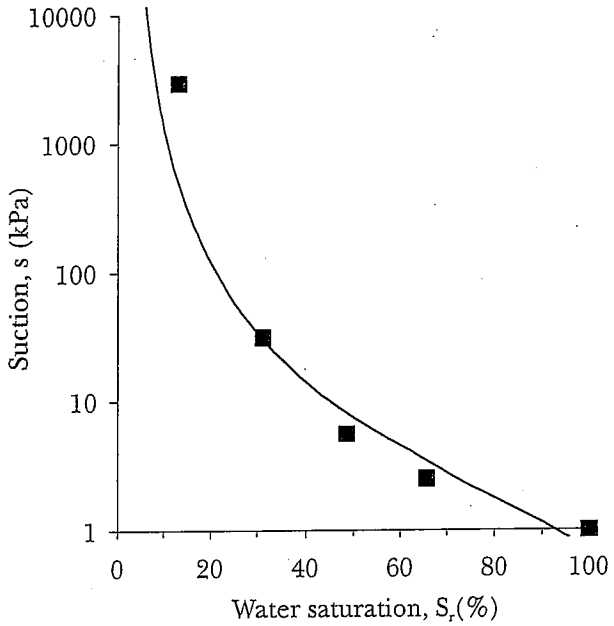

Fig. 5 – Unsaturated soil test: retention curve of the sand sample.

Fig. 5 – Prova su terreno non saturo: curva di ritenzione del campione di sabbia.

ied, most microstructural and mineralogical complicating features can be neglected when interpreting both water retention and electrical data. Nevertheless attention should be paid to hysteretical effects in non monotonous hydraulic paths, that are certainly important for water retention and could be non negligible as well for the electrical conductivity – saturation degree relation. Therefore, a possible interpretation of electrical measurements in terms of suction shall take into account hydraulic history. It is of some interest as well noticing that, since the transport mechanisms causing water and electrical charges to flow are different, non zero electrical conductivities could be obtained as well below irreducible water saturation.

P and S-waves traces measured during the test are shown in figure 6: a good quality of the results can be noticed allowing for a reliable first arrival picking in all saturation conditions and showing a coherent difference in the velocity of the two waves with almost doubled P wave velocities (please notice the different time scales in the two plots). Wave velocities evaluated from the above traces are reported in figure 7 showing trends that are similar to those published by WU *et al.* [1984] and QIAN *et al.* [1991; 1993], that adopted a similar sample preparation technique. As the S-wave velocities are concerned, moderate differences with saturation degrees are observed (Fig. 7). These minor differences can not be explained solely on the basis of the variation of apparent density hence it is necessary to postulate an influence of matric suction. As suction contributes to stiffen the material, it increases as well the S-wave velocity. Indeed, results show systematically decreasing velocities when passing from S_r = 30 % to saturation, that is to say from a matric suction of about 30 kPa to nil. WU *et al.* [1984] proposed an empirical equation to predict the optimum degree of saturation (S_{opt}) corresponding to the peak of the velocity for freshly remoulded specimens. On behalf of this equation and on the basis of the physical properties of the sample, the S_{opt} of the present study would be equal to 8%; anyway, no velocity peaks around this value were found, since no measurements were performed at this saturation degree.

On the contrary, propagation of the P-wave depends both on the mechanical properties of the soil and the stiffness of the pore fluid. Although an adequate interpretation of the evolution of the P-wave velocity with the degree of saturation is more complex (see e.g. COSENTINI, 2006 and CONTE *et al.*, 2009 for a comprehensive formulation), its sharp increase close to complete saturation can be appreciated. Indeed the arrival time of the P wave drastically decreases from 90 % to about 100% of saturation (Fig. 6).

It is interesting to notice that results published by CHO and SANTAMARINA [2001] for a similar test show a different dependency of waves velocity from the degree of saturation, with higher values in the low saturation range. However their study was performed on originally saturated samples that were progressively dried. CHO and SANTAMARINA [2001] explain the differences between their results and

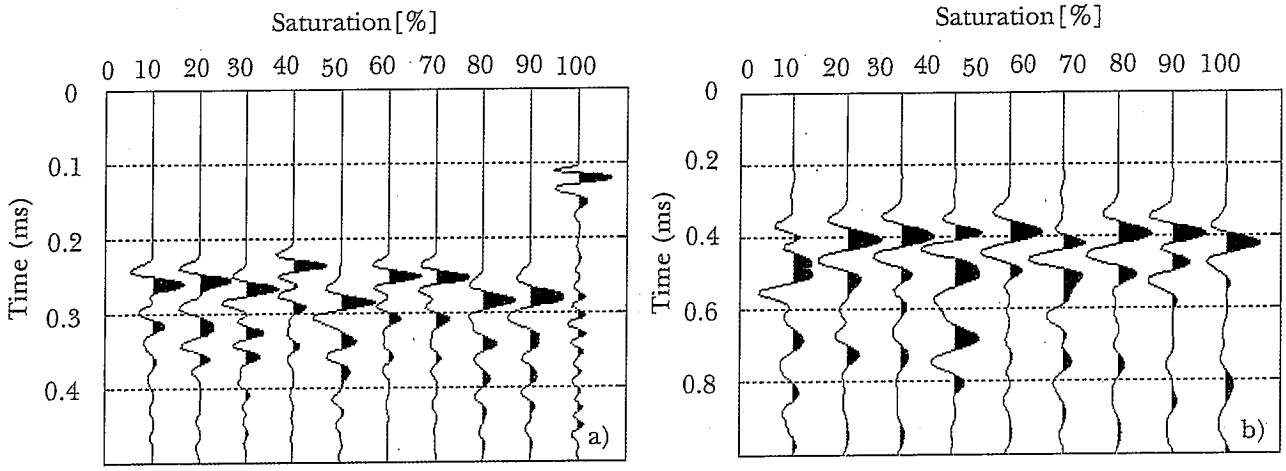

Fig. 6 – Unsaturated soil test: examples of received traces for compressional (a) and shear (b) waves against water saturation degree.

Fig. 6 – Prova su terreno non saturo: esempi delle tracce delle onde di compressione (a) e di taglio (b) a diversi valori del grado di saturazione.

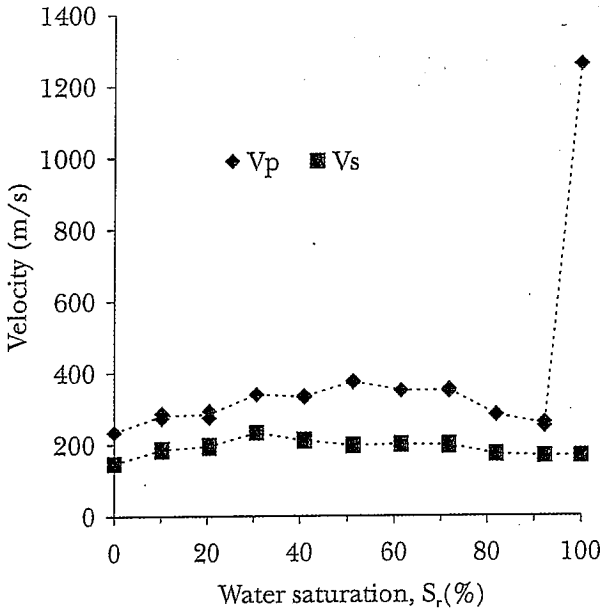

Fig. 7 – Unsaturated soil test: seismic wave velocities against water saturation degree.

Fig. 7 – Prova su terreno non saturo: velocità delle onde sismiche in funzione del grado di saturazione.

the ones of WU *et al.* [1984] and of QIAN *et al.* [1991; 1993] in terms of effects of the drying process.

4. Oedometer Test

Tests have been performed to evaluate the possibility of using ERT to monitor compression and swelling under mechanical loads, and therefore the variation of porosity during oedometer tests. The oedometer tests have been performed on a preconsolidated (100 kPa) kaolinite homogeneous sample saturated with tap water. The limited specific surface and cation exchange capacity of kaolinite generate a very moderate surface conductivity, hence the evolution of the electrical conductivity can be solely related to changes in porosity and tortuosity. A progressive reduction of conductivity was documented during compression, reflecting the reduced void space available for current flow; while the opposite occurred during swelling (Fig. 8). The dependence of the electrical conductivity on load and load history reflects the mechanical response of the sample during loading and unloading. As expected, under increasing effective stresses the electrical conductivity σ_T progressively reduces. Load removal inverts the trend, but the initial conductivity values are not recovered because of the irreversible mechanical behavior. It is of interest to notice that, when approaching and trespassing the preconsolidation stress, the 'knee' on the stress – electrical conductivity curve appears to be more pronounced than the one on the stress – void ratio curve.

In figure 9 the settlement and the average electrical conductivity during a single load step are reported. In the first part of the process, when consolidation is occurring, the settlement increases and the electrical conductivity consistently decreases. Nevertheless, when secondary compression comes in place, the average electrical conductivity experiences a limited increase. This evidence was found to occur during all the loading cycles. A deeper interpretation of the electrical data of the secondary phase, here not attempted, could therefore possibly help in interpreting fabric changes associated to secondary compression. In the literature, those have been attributed alternatively to wa-

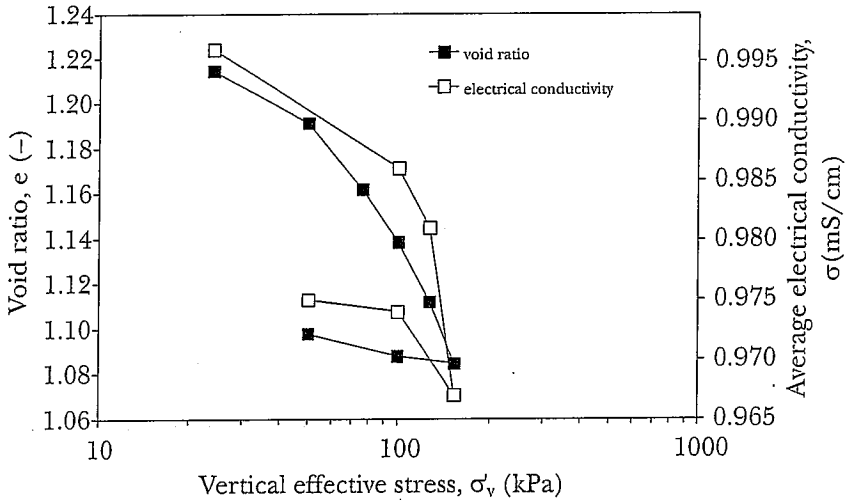

Fig. 8 – Oedometer test: vertical effective stress – void ratio curve (black square) and vertical effective stress - average electrical conductivity curve (white squares). Data refer to measurements taken 24 hours after imposing the load.
Fig. 8 – Prova edometrica: diagramma della tensione verticale efficace in funzione dell'indice dei vuoti (quadrati neri) e della tensione verticale efficace in funzione della conducibilità elettrica media (quadrati bianchi). Dati riferiti a misure eseguite a 24 ore dall'applicazione del carico.

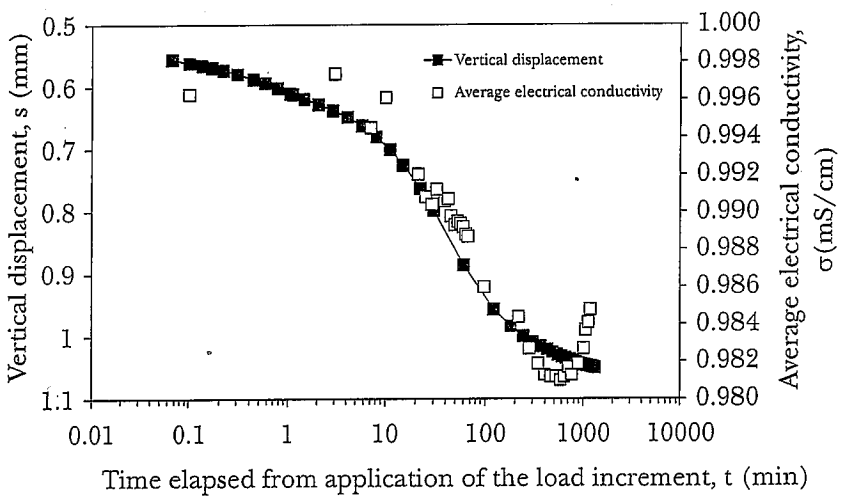

Fig. 9 – Oedometer test: time evolution of the vertical settlement (black squares) and of the average electrical conductivity (white squares) after application of a load increment.
Fig. 9 – Prova edometrica: evoluzione temporale del cedimento verticale (quadrati neri) e della conducibilità elettrica media (quadrati bianchi) durante un gradino di carico.

ter transfer from intra-aggregate to inter-aggregate porosity (as proposed for instance by DE JONG, 1968 and more recently by NAVARRO and ALONSO, 2001); or to the rearrangement of aggregates induced by the same physical mechanisms governing soil consolidation [e.g. WANG and XU, 2007], in accordance with a constant ratio between the compression index c_c and the secondary compression index c_α [MESRI and GODLEWESKI, 1977]. A better way to interpret these experimental results would then rely on electrical relationships that could take into account the distribution of pore sizes in a more complex form than Archie's law. Possible models are those based on effective medium approximations (for their review see e.g. SEN, 1997), where it is assumed that the porous medium is composed by a mixture of two or more different materials, each characterised by its own porosity and electrical conductivity; or to models considering electrical anisotropy.

Local conductivity changes during consolidation are not always simple to interpret. These observations could be due to the fact that the conductivity changes are small and below the resolution of the instrument. When clearly detectable, local conductivity decrease can actually be related to different consoli-

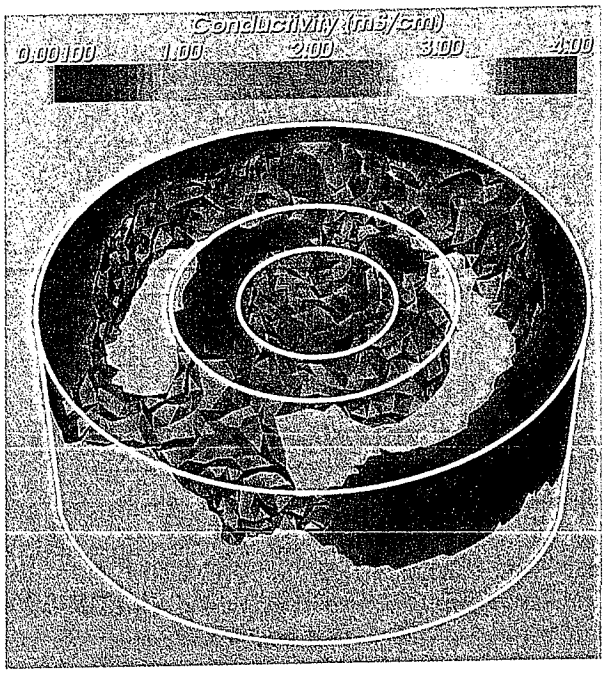

Fig. 10 – Oedometer test: differential image of tomography reconstructions immediately before and after the application of a load increment. Only the mesh elements where $\Delta\sigma > 10^{-3}$ mS cm^{-1} are represented.
Fig. 10 – Prova edometrica: immagine differenziale della ricostruzione tomografica immediatamente prima e dopo l'applicazione del gradino di carico. Sono rappresentati solo gli elementi della mesh con variazione di conducibilità elettrica $\Delta\sigma > 10^{-3}$ mS cm^{-1}.

dation degrees inside the sample. In figure 10, a differential image obtained immediately after the application of a load step is reported. For this oedometer test drainage was allowed only from the sample top. The figure shows the difference between the electrical conductivity immediately before imposing the load and the one just after the application of the load. A threshold in the representation ($\Delta\sigma$ = 0.001 mS/cm) has been set so to document large electrical resistivity changes within the sample. The conductivity results show portions of the specimens that merge towards the concentric rings that operate as drainages, in a complex flow and consolidation conditions.

5. 3D diffusion test

An experiment has been designed in order to induce a 3D diffusion process in a saturated soil sample. Since the diffusion of salts in soils produces changes in the water electrical conductivity, ERT can be used for determining the distributions of the solute by non-invasive and non-destructive measurements. A tap water saturated homogeneous Ticino sand sample (30% relative density) was placed inside the cell. Ticino sand is a virtually monogranular quartz sand (mean particle size of 0.5 mm) with well rounded particles. Quartz minerals possess an exceptionally large resistivity, so that equation [1] is expected to be accurate: in absence of deformations, any changes in the conductivity of the sample can be directly related to changes in the pore fluid properties and hence, for this particular test, to chemical concentration.

Chemical diffusion was induced by placing a localized saline source (NaCl grains) on the top of the sample (Fig. 11). The use of pure NaCl assures a constant concentration condition, in which the concentration is equal to salt solubility; hence the process can be modeled straightforwardly to compare the monitoring with an external benchmark. Tomography data have been acquired at different time intervals from the beginning of the test. The acquisition of a single set of measurements can be performed in a few seconds; then, a short sampling time allows a stationary interpretation of each image providing an instantaneous picture of the monitored process at different time intervals. For the inversion a damping factor equal to 1×10^{-4} has been used. Indeed, since gradients are more pronounced in this test an high value of the damping factor (as used in the previous tests) would artificially smooth the image

An example of reconstruction after 75 minutes from the beginning of the test is presented in figure 12. The presence of the higher conductivity area at the top of the sample, corresponding to the position of the imposed source, can be appreciated. The diffusive flux appears almost perfectly hemispherical due to the homogeneity of the sample.

Figure 13 shows some images of a cross section of the sample (section AA in Fig. 11) passing through the source and the center of the cell obtained at different times. The images refer to first 90 minutes of chemical diffusion. This time interval is not large enough to obtain the homogeneization of the concentration within the soil sample, since the diffusion process is itself quite slow: however, these results can give an important insight about the ability of the measuring technique in identifying the diffusive chemical front during transient processes. Images clearly represent the saline solution diffusing inside the soil sample as the conductivity gradually increases below the source.

Figure 14 reports the trends of electrical conductivity along line D1 (Fig. 11) placed at 0.25 cm below the source, for the entire duration of the test. It can be noticed a gradual increase of conductivity, which is initially concentrated in the vicinity of the source but subsequently spreads laterally until complete homogenization of the upper part of the sample.

In interpreting this experiment, the electrical conductivity of the pore water, σ_w, has been related to the salt concentration by means of an empirical cubic expression [MUSSO and ROMERO, 2005], al-

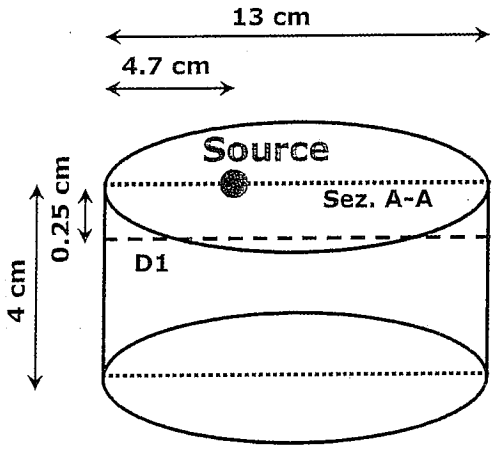

Fig. 11 – Diffusion test: scheme of test setup for the 3D salt diffusion.
Fig. 11 – Prova di diffusione: schema dell'allestimento della prova per la diffusione 3D di un sale.

Fig. 12 – Diffusion test: ERT reconstruction after 75 minutes from the beginning of the diffusion test.
Fig. 12 – Prova di diffusione: ricostruzione ERT a 75 minuti dall'inizio della prova di diffusione.

though theoretical relationships could be used [e.g. ROBINSON and STOKES, 1968].

It has then been assumed that the tortuosity of the soil medium affects the transport of ions in the same manner when electrical or chemical gradients are acting, in line with the Nernst –Townsend – Einstein relationship [HOLMES, 1962]. As a consequence, the electrical conductivity of the soil, σ_T can be related to σ_w in the following manner:

$$\sigma_T = \tau \sigma_w \qquad (3)$$

τ being an empirical tortuosity coefficient, accounting for porosity and other factors.

Similarly, the mass balance of the dissolved salt has been written as:

$$n \frac{\partial c}{\partial t} D^* \nabla^2 c = 0 \qquad (4)$$

where c is the salt concentration, $D^* = \tau D$ is the effective diffusion coefficient of the salt in the soil and D the molecular diffusion coefficient of the salt in water.

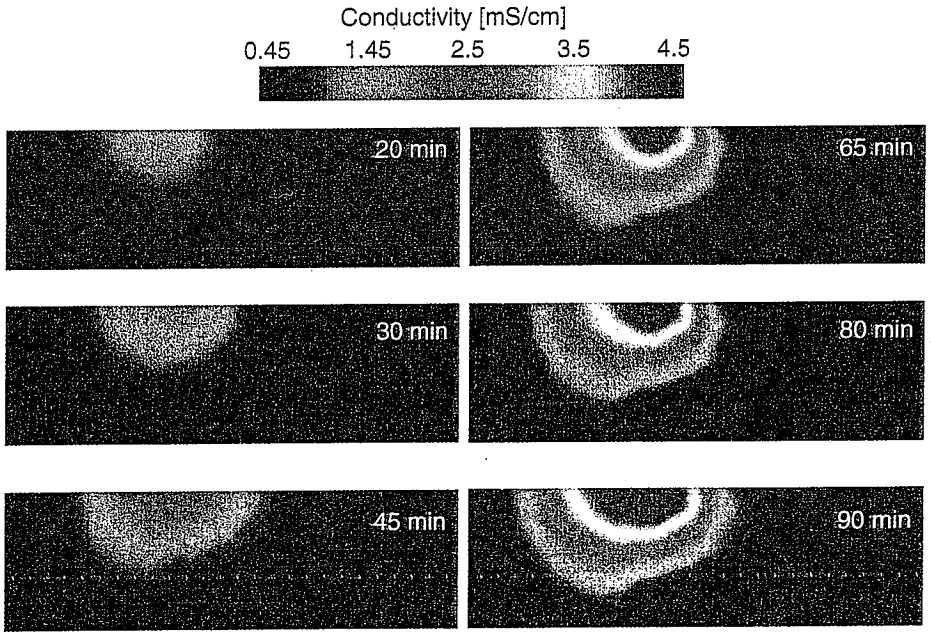

Fig. 13 – Diffusion test: snapshots of a cross section of the ERT reconstruction at different times from the beginning of diffusion.
Fig. 13 – Prova di diffusione: istantanee di una sezione verticale delle ricostruzioni ERT in tempi successivi dall'inizio del processo.

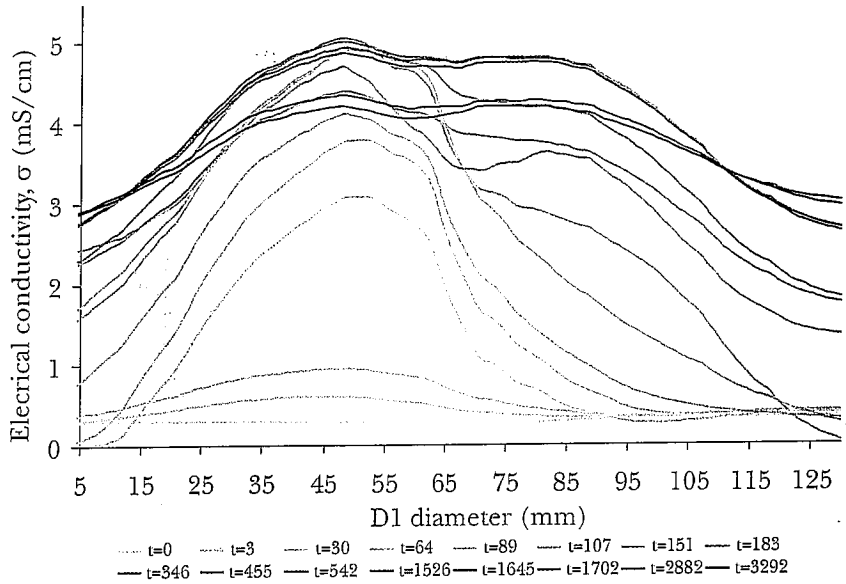

Fig. 14 – Diffusion test: conductivity values along D1 diameter at different times (t in minutes).
Fig. 14 – Prova di diffusione: valori di conducibilità lungo il diametro D1 in tempi successivi (t in minuti).

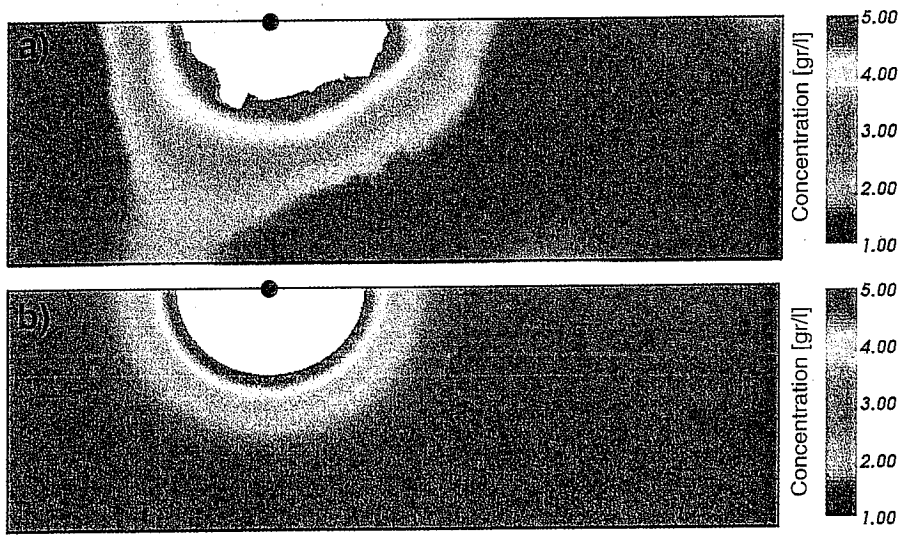

Fig. 15 – Diffusion test: cross section of salt concentration at 45 min: a) ERT reconstruction b) FEM simulation.
Fig. 15 – Prova di diffusione: sezione verticale della concentrazione di sale a 45 min: a) ricostruzione ERT b) simulazione FEM.

The diffusion process has been simulated with a commercial FEM program (Comsol®) and results have been compared to the experimental distribution of concentrations at the different times during the evolution of the diffusion process. The procedure was repeated to estimate the value of the effective diffusion parameter that minimized the scatter between experimental and simulation data, which was found to be equal to $3\ 10^{-10}$ m^2/s, a value that compares quite well with literature data. MITCHELL and SOGA [2005] report that, for different chemicals and soils, D^* ranges between $2\ 10^{-10}$ and $2\ 10^{-9}$ m^2/s. Moreover, since the diffusion coefficient of NaCl in pure solutions is equal to $1.6\ 10^{-9}$ m^2/s, [ROBINSON and STOKES, 1968], it is found $\tau = 0.19$. It can be noted that, if Archie's law was used instead of equation (3), a value $m = 1.8$ would have been found.

In figure 15 a comparison between the experimental data and the numerical simulation after 45 minutes from the beginning of the test is reported. The numerical simulation compares promisingly well with the tomography reconstruction both in the shape of the diffusive front and in the values of the concentration along it. Sensitivity problems are partially observed in the parts of the sample having higher conductivity gradients, particularly near the diffusive source where the concentration locally jumps from the one of the pure salt to the one

inside the specimen and cannot be exactly recovered by electric tomography (the white zone omitted in Fig. 15). This is a limitation of the regularized inversion; however the result presented underlines how the diffusive front is correctly managed by ert reconstruction. In particular partial differences in the shape of the front if compared to the numerical simulations are mostly related to actual inhomogeneities in the sample than to sensitivity problems. Indeed, local heterogeneities in the soil sample are expected due to preparation by compaction. This observation underlines the potentiality of ERT in monitoring diffusion processes in natural soil samples where preferential path can play a fundamental role in the comprehension of actual diffusion processes.

Conclusions

Experimental results concerning the use of the electrical resistivity tomography to identify saturation changes, mechanical consolidation and saline diffusion in laboratory samples have been presented. 3D ERT appeared to be a capable technique for imaging samples heterogeneities. Average and local variations of the reconstructed conductivity values were interpreted in light of simple models of the soil electrical conductivity, assuming water as the only electrically conductive phase of the soil. As for changes of the saturation degree, an example of the calibration of Archie's law parameters for a fine sand sample at increasing degree of saturation has been presented and compared with the concomitant evolution of the elastic wave velocities. For consolidation, interesting results were found for what concerns the consequences of the load history on the electrical behavior. As well, in a number of cases the possibility to use ERT to identify areas of higher consolidation has been found. As for the diffusion of saline solutions, promising results were found regarding the possibility of estimating the values of the transport parameters on the basis of the reconstructed conductivity values.

Acknoledgements

The authors acknowledge Mr. Tomas Perez and Dr. Enrique Romero of UPC (Barcelona) for the fundamental contribution of in the design of the oedometer cell, and for its construction; and Ms Elisa Bogino for performing one dimensional compression tests.

References

ARCHIE G.E. (1942) – *The electrical resistivity log as an aid to determining some reservoir characteristics.* Trans AIME, 146, pp. 54-63.

ASTM STANDARD (1997) – *D 5298-94 "Standard test method for measurement of soil potential (suction) using filter paper".* Annual book of ASTM standard, ASTM International.

BERRYMAN J.G. (1995) – *A Handbook of Physical Constants.* American Geophysical Union, Washington D.C.

BINLEY A., SHAW B., HENRY-POULTER S. (1996) – *Flow pathways in porous media: electrical resistance tomography and dye staining image verification.* Meas. Sci. Technol., 7, pp. 384-390.

BLEWETT J., MCCARTER W.J., CHRISP T.M., STARRS G. (2001) – *Monitoring sedimentation of a clay slurry.* Géotechnique, 51, n. 8, pp. 723-728.

CHO G.C. and SANTAMARINA J.C. (2001) – *Unsaturated particulate materials – Particle-Level studies.* J. Geot. Geoen. Eng., 127, n.1, pp. 84-96.

COMINA C., FOTI S., LANCELLOTTA R., MUSSO G., BORSIC A. (2005) – *Imaging heterogeneities and diffusion in sand samples.* Proc. 11th International Conference of the International Association of Computer methods and Advances in Geomechanics IACMAG2005, Torino, 2, pp. 27-34.

COMINA C., FOTI S., MUSSO G., ROMERO E. (2008) – *EIT oedometer – an advanced cell to monitor spatial and time variability in soil.* Geotechnical Testing Journal, ASTM, 31, n. 5, pp. 404-412.

CONTE E., COSENTINI R.M., TRONCONE A. (2009) – *Shear and dilatational wave velocities for unsaturated soils.* Soil Dynamics and Earthquake Engineering, 29, n. 9, pp. 946-952.

COSENTINI R.M. (2006) – *La propagazione delle onde elastiche in mezzi porosi non saturi.* PhD. Thesis, Università Mediterranea di Reggio Calabria, Italy (in Italian).

DAMASCENO V., FRATTA D., BOSSCHER P. J. (2009) – *Development and validation of a low-cost electrical resistivity tomographer for soil process monitoring.* Canadian Geotechnical Journal, 46, n. 7, pp. 842-854.

DE JONG G.J. (1968) – *Consolidation models consisting of an assembly of viscous elements or a cavity channel network.* Géotechnique, 18, pp.195–228.

HOLMES P.J. (1962) – *The electrochemistry of semiconductors.* Academic Press, London, England.

KAMON M., ENDO K.E., KATSUMI T. (2003) – *Measuring the k – S – p relations on DNAPLs migration.* Engineering Geology, 70, pp. 351-363.

LIONHEART W.R.B., KAIPIO J., MCLEOD C.N. (2001) – *Generalized optimal current patterns and electrical safety in EIT.* Physiol. Meas., 22, pp. 85-90.

MCCARTER W.J., DESMAZES P. (1997) – *Soil characterization using electrical measurements.* Géotechnique, 47, n.1, pp. 179-183.

McCARTER W.J., BLEWETT J., CHRISP T.M., STARRS G. (2005) – *Electrical property measurements using a modified hydraulic oedometer*. Canadian Geotechnical Journal, 42, pp. 655-662.

MENKE W. (1989) *Geophysical Data Analysis: Discrete Inverse theory*. International Geophysics Series, San Diego, Academic Press.

MESRI G., GODLEWSKI P. M. (1977) – *Time- and stress compressibility interrelationship*. J. Geotech. Eng. Div., Am. Soc. Civ. Eng., 103, n. 5, 417-430.

MITCHELL J.K., SOGA K. (2005) – *Fundamentals of soil behaviour*. John Wiley and Sons, New York.

MUALEM Y., FRIEDMAN P. (1991) – *Theoretical prediction of electrical conductivity in saturated and unsaturated soil*. Water resources research, 27, pp. 2771-2777.

MUSSO G., ROMERO E. (2005) – *Chemio-mechanical behaviour of high-density bentonites. Imbibition and diffusion tests*. Advances in Understanding Engineered Clay Barriers – Alonso & Ledesma (eds.), pp. 283-291.

NAVARRO V., ALONSO E. (2001) – *Secondary compression of clays as a local dehydration phenomena*. Géotechnique, 51, n.10, pp. 859-869.

PFANNKUCH H.O. (1969) – *On the correlation of electrical conductivity properties of porous systems with viscous flow transport coefficients*. Proc. IAHR 1st Int. Symp. Fundamentals of Transport Phenomena in Porous Media, Haifa.

QIAN X., GRAY D.H., WOODS R.D. (1991) – *Resonant column tests on partially saturated sands*. Geotech. Testing J., 14, n.3, pp. 266-275.

QIAN X., GRAY D.H., WOODS R.D. (1993) – *Voids and granulometry: Effects on shear modulus of unsaturated sands*. J. Geotech. Engrg., ASCE, 119, n. 2, pp. 295-314.

ROBINSON R.A., STOKES R.H. (1968) – *Electrolyte solutions*. Buttherworths, London.

SANTAMARINA J.C., KLEIN K.A., FAM M.A. (2001) – *Soils and Waves*. John Wiley and Sons, New York.

SEN P. N. (1997) – *Resistivity of partially saturated carbonate rocks with microporosity*. Geophysics, 62, n. 2, pp. 415-425.

SHACKELFORD C.D., MALUSIS M.A., MAJESKI M.J., STERN R.T. (1999) – *Electrical conductivity breakthrough curves*. Journal of Geotechnical and Geoenvironmental Engineering, 125, n. 4, pp. 260-270.

SOMERSALO E., CHENEY M., ISAACSON D. (1992) – *Existence and uniqueness for electrode models for electric current computed tomography*. SIAM J. Appl. Math, 52, pp. 1023-1040.

TARANTOLA A. (2005) – *Inverse problem theory and methods for model parameter estimation*. SIAM, Philadelphia, USA.

VAN GENUCHTEN M. (1980) – *A close-form equation for predicting the hydraulic conductivity of unsaturated soils*. Soil Sci. Soc. Am. J., 44, pp. 892-898.

WAXMAN M. H., SMITS L. J. M. (1968) – *Electrical Conductivities in Oil-Bearing Shaly Sands*. Soc. Pet. Eng. J., 8, pp. 107-122.

WANG Y. H., XU D. (2007) – *Dual porosity and secondary consolidation*. J. of Geotech. and Geoenv. Engrg., ASCE, 133, n. 7, pp. 793-801.

WU S., GRAY D.H., RICHART F.E. JR. (1984) – *Capillary effects on dynamic modulus of sands and silts*. J. Geotech. Engrg., ASCE, 110, n. 9, pp. 1188-1203.

YEUNG A.T. (1990) – *Coupled flow equations for water, electricity and ionic contaminants through clayey soils under hydraulic, electrical and chemical gradients*. J. of Non Equilibrium Thermodynamics, 15, n. 3, pp. 247-267.

La Tomografia Elettrica come strumento di monitoraggio in laboratorio

Sommario

La Tomografia Elettrica di Resistività (ERT) è una tecnica di indagine che si è dimostrata efficace per la caratterizzazione dei terreni e il monitoraggio in diverse applicazioni in situ. In particolare, l'ERT è spesso usata in geofisica per la ricostruzione dei profili geologici e per il monitoraggio del flusso di contaminanti, fornendo indicazioni sulla dispersione spaziale e sulla localizzazione della sorgente inquinante. Risultati interessanti sono stati recentemente ottenuti anche in laboratorio, mostrando la potenzialità dell'ERT come strumento complementare nella caratterizzazione dei campioni di terreno e nel monitoraggio delle prove.

I metodi ERT sono relativamente economici e veloci in termini di acquisizione dei dati. I vantaggi della tecnica si basano sul fatto che la conducibilità elettrica può essere messa in relazione con le proprietà fisico-chimiche del complesso acqua-terreno (concentrazione delle specie ioniche, porosità, tortuosità, superficie specifica, capacità di scambio cationica). In linea di principio, i risultati ERT possono essere usati non solo per scopi di imaging, ma possono anche essere interpretati da un punto di vista quantitativo, come supporto nella caratterizzazione dei parametri di trasporto.

In questo contesto, il presente articolo riporta i risultati di alcune prove di laboratorio studiate per esplorare le potenzialità della tecnica ERT 3D con riferimento a fenomeni di interesse per l'ingegneria geotecnica. Le prove sono state eseguite in una cella edometrica innovativa, attrezzata sia per la esecuzione della tomografia elettrica 3D sia per la misura della velocità delle onde di compressione e di taglio, le quali possono fornire uno strumento di monitoraggio indipendente. Si riportano i risultati relativi a: variazione del grado di saturazione, consolidazione mono-dimensionale, monitoraggio del processo di diffusione di sali.